Repulsive interaction between coplanar cracks in the double-cantilever geometry

Kai-tak Wan
Department of Physics and Astronomy, University of Maryland, College Park, Maryland 20742

Brian R. Lawn and Roger G. Horn
Ceramics Division, National Institute of Standards and Technology, Gaithersburg, Maryland 20899

(Received 30 September 1991; accepted 3 February 1992)

Experiments on thin mica sheets are used to demonstrate that coplanar cracks in double-cantilever beam specimens do not universally attract each other, as conventionally portrayed, but, at long range, actually repel. An elasticity analysis explains the repulsion in terms of a compression zone, ≈0.35 times the beam half-thickness ahead of the crack tip, generated by bending moments from the cantilever arms on the remaining specimen section.

I. INTRODUCTION

The stress field around the tip of a mode I crack in an ideal infinite Hookean continuum solid is essentially tensile.[1] When two coplanar cracks approach each other the superposition of the tensile fields manifests itself as an "attraction",[2–4] with a strong tendency to coalesce. The attraction may be sufficiently strong to effect coalescence between cracks on adjacent planes, via mixed-mode out-of-plane deflections.[5,6] It is therefore not unnatural to generalize the expectation of mutual attraction to all crack geometries.

However, as we shall show, this generalization does not necessarily extend to specimens with finite dimensions. An illustrative example of specific interest to us here is the double-cantilever beam (DCB) crack specimen. Elasticity analyses of the DCB specimen[7,8] indicate the existence of a compression zone some distance ahead of the crack tip. The perturbing effect of the stress-free beam surfaces alters not only the magnitude of the crack stresses but also the sign, so that approaching cracks may actually repel.

We investigate this possibility by observing the interaction of coplanar cracks at healed interfaces in DCB specimens of muscovite mica. We find that the cracks repel until, at a mutual tip-to-tip approach of about one-half the thickness of one beam, they abruptly coalesce. On unloading the specimen the original cracks re-form from the coalesced configuration, again abruptly but with hysteresis. The hysteretic instability alludes to the existence of an energy barrier which must be overcome before the two cracks merge. A theoretical account of the observations is given using an approximate stress analysis based on a modification of one of the earlier analyses.[8]

II. EXPERIMENT

Specimens of muscovite mica were cut into slabs 25 × 10 mm by 50 μm. Each specimen was cleaved into two sheets of near-equal thickness and near-atomic smoothness. During the cleavage, some inadvertent mica flakes of diameter 1 to 5 μm dislodged from the specimen edges fell onto the surfaces. The two mica sheets were then placed back into adhesive contact after a rotation of 10 to 20° to form a healed (misoriented) interface.[9] The trapped flakes acted as sources of local crack opening displacements, thereby forming a number of well-defined internal penny cracks at the recontacted interface.

After formation of the internal cracks, a steel wedge of thickness 50 μm was inserted into the healed interface so as to run a straight DCB crack toward the internal pennies, Fig. 1. The specimen was mounted into a fixture that enabled controlled insertion or withdrawal of the wedge.[9,10] In their fixed-displacement configurations, both the DCB primary crack and the internal penny cracks are intrinsically stable, allowing for a steady approach to the point of coalescence. The wedge-loading fixture was mounted onto the stage of an inverted reflection microscope, to allow photographs to be taken at prescribed intervals during the loading-unloading cycles. All such tests were run in laboratory air, and sufficient time was allowed between wedge-loading increments for the system to equilibrate.[9] An *in situ* record of the crack front and wedge position was also made on a

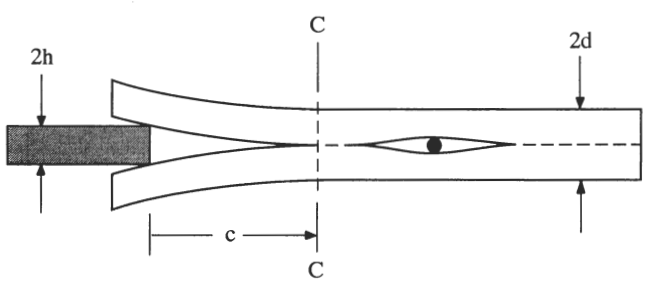

FIG. 1. Schematic of wedge-loaded mica DCB crack specimen containing a coplanar interval penny crack.

video recorder to enable more detailed analysis of the crack-interaction evolution.

III. RESULTS

A typical crack-interaction sequence is shown in Fig. 2. Two-beam Fizeau interference between the separated walls provides the means for observing the crack distortions and locating the crack fronts (by extrapolation to zero-order dark fringe.[9,10] The DCB crack front is straight over almost all of the sample width. Figure 2(a) shows the DCB crack at left approaching an internal penny crack at right. In this frame the fringes at the DCB crack are straight and parallel while those at the internal crack are concentric about a small but visible mica particle, indicating no interaction as yet. On further inserting the wedge, Figs. 2(b) and 2(c), the DCB crack front wraps around the penny crack, distorting the shape of the latter. The fringes along the horizontal center line between the two cracks are progressively compressed, signifying a mutual repulsion. The curvature of the

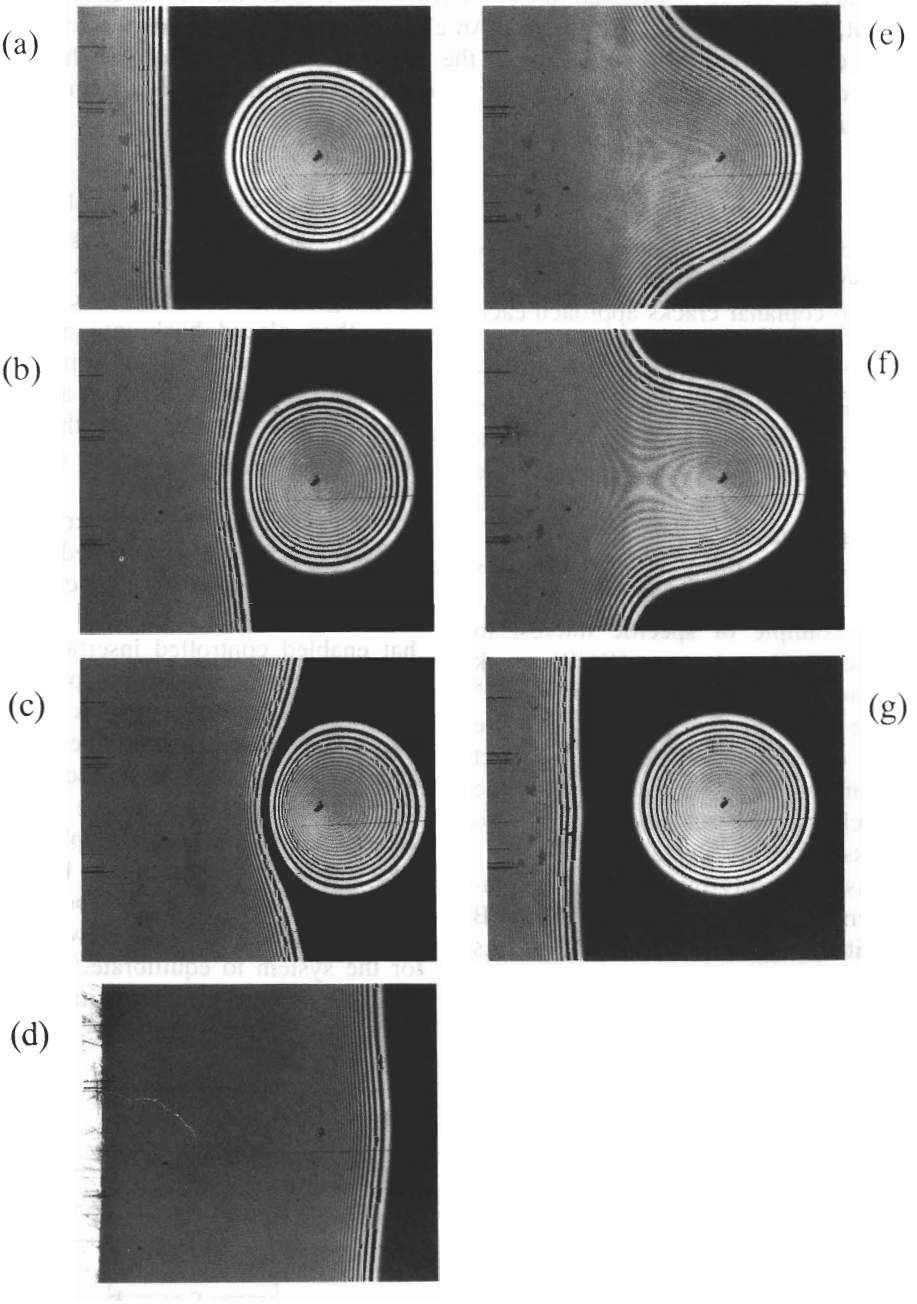

FIG. 2. Series of micrographs showing the interaction between a straight DCB crack and an internal coplanar penny crack in muscovite mica sheet. Wedge position relative to trapped particle in penny crack center: *insertion*: (a) −1.90 mm, (b) −1.60 mm, (c) −1.26 mm, and (d) −1.05 mm (wedge visible at left); *withdrawal*: (e) −1.89 mm, (f) −1.94 mm, and (g) −1.99 mm. Note compression of the fringe pattern as cracks approach, and hysteresis during the loading-unloading cycle. Dimensions $2d = 50$ μm, $2h = 50$ μm (cf. Fig. 1). Width of field 1.63 mm.

DCB crack front, the asymmetry of the penny crack, and the spatial density of fringes in the vicinity of the mutually approaching fronts continue to increase until an instability is reached, at which point coalescence suddenly occurs, Fig. 2(d). Still further advancement of the wedge causes the DCB crack to propagate as a single entity, with an ever-increasingly straight front. At this point the wedge displacement is reversed. The DCB crack attempts to close, Figs. 2(e) and 2(f), but is restrained by the interfacial mica particle. It is as if the curved crack front possesses a kind of line tension. Ultimately, the neck connecting the DCB and penny "ruptures", restoring the original crack configuration, Fig. 2(g).

This hysteretic sequence repeats itself in subsequent propagation-healing cycles. The same sequence of events is observed at many other penny cracks in the same specimen. We find that the distance of closest approach between the interacting crack fronts prior to coalescence is on the order one-half of one beam thickness, independent of the diameter of the penny cracks.

Conventional fracture mechanics allows us to quantify the crack repulsion effect observed in Fig. 2. The mechanical-energy-release rate G for an isolated crack in the DCB geometry is[1,11]

$$G = 3Ed^3h^2/4c^4 \tag{1}$$

with E Young's modulus (170 GPa for mica parallel to the crack plane), $2d$ the double-beam thickness, $2h$ the wedge thickness, and c the DCB crack length. Now this analysis strictly applies for a straight-fronted crack, but if we measure c along the horizontal center line bisecting the penny we may retain Eq. (1) as a useful (if greatly exaggerated) bound, G' say. Accordingly, Fig. 3 plots G' as a function of wedge position relative to the center of the penny crack. When the two cracks are far apart, the DCB crack is in equilibrium at $G' = G = W$, where $W = 250\ \text{mJ}\cdot\text{m}^{-2}$ is the interface energy for mica in air.[12] The apparent G' value increases strongly to $\approx 1500\ \text{mJm}^{-2}$ over a wedge displacement of ≈ 1 mm before abrupt crack coalescence (AA′). Thereafter, G' rapidly restores to its equilibrium value. On reversing the wedge, G' diminishes steadily to the point of separation (BB′), well to the left of the original coalescence position. The hysteresis in the cycle is evident.

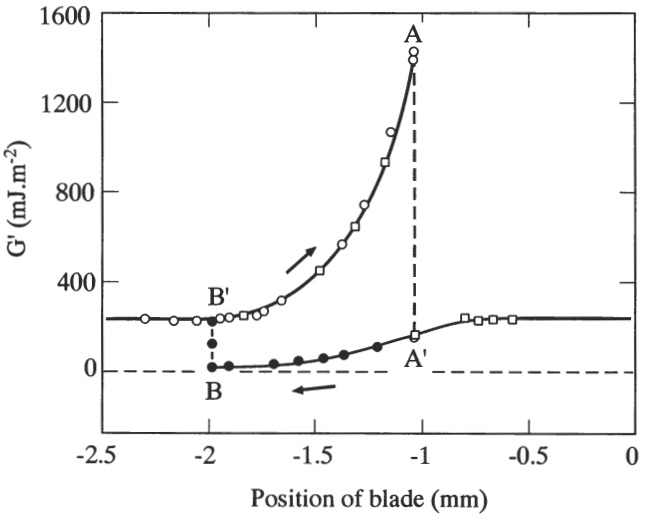

FIG. 3. Plot of apparent mechanical energy release rate G' for DCB crack in mica as function of wedge position relative to the trapped particle. Open circles denote first loading half-cycle, closed circles first unloading, and open squares subsequent reloading. Vertical dashed line AA′ denotes the position at which the DCB and penny cracks coalesce and BB′ the position at which they separate. $G' = G = W = 250\ \text{mJ}\cdot\text{m}^{-2}$ is equilibrium level for crack propagation in air.

IV. ANALYSIS

To analyze the results of the previous section, we need to determine the crack stress field of the DCB crack and the modification of this field due to interaction with the second crack. There is no closed-form solution that allows properly for the stress-free outer beam boundaries in the DCB geometry. Accordingly, we adopt an approximate procedure to estimate this field and thence to evaluate the consequent mutual interaction in the presence of the second crack.

Our procedure follows from an elasticity analysis of the DCB crack system by El-Senussi and Webber.[8] The two cantilever beams are regarded as attached to the uncracked section to the right of the plane CC in Fig. 1. Stresses on the plane $x = 0$ resulting from the bending moments on the beams are approximately in the linear distribution of Fig. 4:

$$\sigma_x(0, y) = \left(3Ehd/2c^2\right)(1 - 2y/d), \quad (0 \leqslant y \leqslant d) \tag{2a}$$

$$= \left(3Ehd/2c^2\right)(1 + 2y/d), \quad (-d \leqslant y \leqslant 0). \tag{2b}$$

The body to the right of the crack tip is now assumed to be a semi-infinite solid rather than a finite strip. This simplification is unlikely to cause serious error for conditions near the center crack plane and reasonably close (on the scale of the beam thickness) to the crack tip. Then one may use the simple stress solution for a concentrated line force on a half-space[13] to evaluate the field. Accordingly, we consider the distributed load to be composed of elemental normal line forces $\sigma_x dy$ acting on the straight boundary at point $-d \leqslant y \leqslant d$ along the section. Each such element induces a purely radial stress field $\sigma_r(r, \theta)$

$$\sigma_r(r, \theta) = -(2\sigma_x dy/\pi r)\cos\theta \tag{3}$$

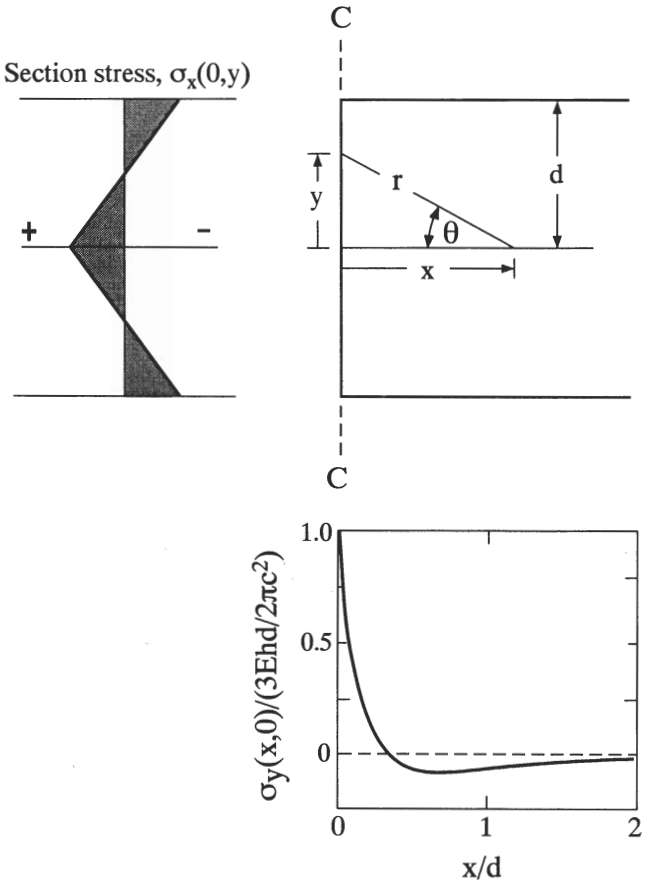

FIG. 4. Normal stress distribution $\sigma_x(0, y)$ (at left) on DCB cross section CC through the crack tip (at right). Ensuing stress distribution σ_y $(x, 0)$ at crack plane ahead of tip (normalized coordinates). Note onset of compression at $0.35 < x/d$.

where r, θ are polar coordinates relative to a field point along the prolongation of the crack plane. Resolving this stress normal to the crack plane and inserting Eq. (2), we may integrate over the end section to obtain the net stress at each point along the crack plane:

$$\sigma_y(x, 0) = -(2/\pi) \int_{-\theta_d}^{\theta_d} \sigma_x(0, y) \sin^2 \theta \, d\theta$$
$$= (3Ehd/2\pi c^2)\{2\theta_d - \sin 2\theta_d - 4 \cot \theta_d [\cos^2 \theta_d - 2\ln(\cos \theta_d) - 1]\} \quad (4)$$

where $\cot \theta_d = x/d$. Figure 4 plots the normalized quantities $\sigma_y(x, 0)/(3Ehd/2\pi c^2)$ as a function of x/d. We see that the stress at the crack tip is tensile immediately ahead of the crack tip but becomes compressive at $x/d \approx 0.35$. The compression reaches a minimum at $x/d \approx 0.68$ and decays asymptotically to zero at $x/d \longrightarrow \infty$.

Thus the embedded penny crack on the separation plane in Fig. 1 will initially experience a compressive field from the approaching DCB crack. Additional work must then be done to push the cracks closer together, resulting in a mutual repulsion. As the wedge drives the DCB crack farther forward the repulsion increases until, ultimately, the two crack fronts enter the near-tip tensile field. Beyond this point the interaction becomes attractive, and the cracks jump into coalescence.

V. DISCUSSION

We have shown experimentally that a strong repulsive interaction exists between coplanar cracks in the DCB geometry. The repulsion is attributed to a compressive component in the stress field ahead of the crack front. Physically, the compression can be regarded as a manifestation of the bending moments exerted by the beam arms on the section CC in Fig. 1, about a "hinge" located at the crack tip. We emphasize that the crack-plane stress distribution in Fig. 4 computed from our model is approximate. It inaccurately represents the field at x/d very small, where a singularity of the form $\sigma_y = x^{-1/2}$ must prevail,[1] and at x/d very large, where the perturbing influence of the beam free surfaces [ignored in Eq. (3)] must become ever stronger. Nevertheless, we may be confident that the model adequately describes the essential feature of main interest here, i.e., the crack-plane compression at intermediate values of x/d.

As already indicated, the hysteresis summarized pictorially in Fig. 2 and graphically in Fig. 3 signifies an energy barrier to coalescence and separation of the coplanar cracks. Thus at close approach, i.e., at separation $\approx d/3$, there are two equilibrium configurations, one stable and the other metastable. On loading, there comes a point where the system would energetically prefer to be in the coalescence state, but is as yet unable to achieve this state because of the mutual repulsion. It is only when the very-near tensile stress fields are ultimately forced to overlap each other that the cracks are able to merge. Similarly, on unloading, the reseparation into individual cracks is impeded by the mutual attraction.

The present findings have implications concerning microcrack toughening. Generally, it is presumed that the shielding is positive; i.e., the field of the primary crack acts to open the microcracks so that any residual internal mismatch stresses may be released, and energy thus absorbed. In the present instance the tensile field about the primary crack front is strongly attenuated by the influence of the free beam surfaces. Hence specimen geometry may be an important factor in microcrack (or even phase transformation) toughening.

ACKNOWLEDGMENTS

The authors are grateful to T-J. Chuang, E. R. Fuller, and S. M. Wiederhorn for stimulating discussions. Funding was provided by the United States Office of Naval Research.

REFERENCES

1. B.R. Lawn, *Fracture of Brittle Solids* (Cambridge University Press, Cambridge, 1992).
2. H. Tada, P.C. Paris, and G.R. Irwin, *The Stress Analysis of Cracks Handbook* (Del Research Corp., Hellertown, PA, 1973).
3. M. Kachanov, Int. J. Solids Structures **23** (1), 23–43 (1987).
4. M. Kachanov and J-P. Laures, Int. J. Fracture **41** (4), 289–313 (1989).
5. M.V. Swain and J.T. Hagan, Eng. Fracture Mech. **10** (2), 299–304 (1978).
6. M.V. Swain, B.R. Lawn, and S.J. Burns, J. Mater. Sci. **9** (2), 175–183 (1974).
7. S.M. Wiederhorn, A.M. Shorb, and R.L. Moses, J. Appl. Phys. **39** (3), 1569–1572 (1968).
8. A.K. El-Senussi and J.P.H. Webber, J. Appl. Phys. **56** (4), 885–889 (1984).
9. K-T. Wan, N. Aimard, S. Lathabai, R.G. Horn, and B.R. Lawn, J. Mater. Res. **5**, 172–182 (1990).
10. D.H. Roach, S. Lathabai, and B.R. Lawn, J. Am. Ceram. Soc. **71** (2), 97–1051 (1988).
11. D.H. Roach, D.M. Heuckeroth, and B.R. Lawn, J. Colloid Interface Sci. **114** (1), 293–294 (1986).
12. K-T. Wan and B.R. Lawn, Acta Metall. **38** (11), 2073–2083 (1990).
13. S. Timoshenko and J.N. Goodier, *Theory of Elasticity* (McGraw-Hill, New York, 1951), pp. 85–96.